Two-Dimensional Materials

How to cite:
International Edition: doi.org/10.1002/anie.202209762
German Edition: doi.org/10.1002/ange.202209762

Vinylene-Linked 2D Conjugated Covalent Organic Frameworks by Wittig Reactions

Yannan Liu[+], Shuai Fu[+], Dominik L. Pastoetter, Arafat Hossain Khan, Yingying Zhang, Arezoo Dianat, Shunqi Xu, Zhongquan Liao, Marcus Richter, Minghao Yu, Miroslav Položij, Eike Brunner, Gianaurelio Cuniberti, Thomas Heine, Mischa Bonn, Hai I. Wang, and Xinliang Feng**

Abstract: Vinylene-linked two-dimensional covalent organic frameworks (V-2D-COFs) have shown great promise in electronics and optoelectronics. However, only a few reactions for V-2D-COFs have been developed hitherto. Besides the kinetically low reversibility of C=C bond formation, another underlying issue facing the synthesis of V-2D-COFs is the attainment of high (*E*)-alkene selectivity to ensure the appropriate symmetry of 2D frameworks. Here, we tailor the *E*/*Z* selectivity of the Wittig reaction by employing a proper catalyst (i.e., Cs_2CO_3) to obtain more stable intermediates and elevating the temperature across the reaction barrier. Subsequently, the Wittig reaction is innovatively utilized for the synthesis of four crystalline V-2D-COFs by combining aldehydes and ylides. Importantly, the efficient conjugation and decent crystallinity of the resultant V-2D-COFs are demonstrated by their high charge carrier mobilities over 10 $cm^2 V^{-1} s^{-1}$, as revealed by non-contact terahertz (THz) spectroscopy.

As a new class of two-dimensional (2D) conjugated polymers (CPs), fully carbon-conjugated V-2D-COFs with extended in-plane conjugated skeletons hold great promise for opto-electronics,[1–4] photoluminescence,[5] photocatalysis[6,7] and energy storage,[8,9] etc. V-2D-COFs synthesized by Knoevenagel polycondensation display significantly enhanced conjugation and chemical stability compared to analogous COFs with imine linkages,[1,10,11] as stimulates the development of this class of materials.[10–12] However, the poorly reversible nature of C=C bond formation makes the synthesis of V-2D-COFs quite challenging, limiting the feasible strategies to only a few reactions, including the Knoevenagel reaction,[3,8,10,11] Aldol-type reaction[13a,b,c,14] and Horner–Wadsworth–Emmons (HWE) polycondensation,[15,16] with a small number of available monomers.[1,4,17] Thereby, it is highly desirable to explore novel synthetic methods for developing crystalline V-2D-COFs. Besides, effective stereoselectivity tuning of *trans/cis*- (*E*/*Z*) C=C bond conformation is important from the standpoint of organic chemistry,[18a,b,19] and it is a prerequisite for achieving well-ordered crystalline V-2D-COFs (Figure S1). Nevertheless, it remains challenging to achieve high *E* selectivity for these reactions with intrinsically low *E*/*Z* selectivity due to the decrease in entropy from a stereoisomerism mixture to a single configuration.

Herein, we report a new protocol for synthesizing unsubstituted V-2D-COFs using the base-catalyzed Wittig reaction between aryl triphenyl phosphonium ylides and aryl aldehydes. The Wittig reaction (Wittig olefination) has been extensively used in organic chemistry to introduce C=C

[*] Dr. Y. Liu,[+] Dr. D. L. Pastoetter, Dr. S. Xu, Dr. M. Richter, Dr. M. Yu, Prof. T. Heine, Prof. X. Feng
Chair of Molecular Functional Materials, Center for Advancing Electronics Dresden (cfaed) and Faculty of Chemistry and Food Chemistry, Technische Universität Dresden
Mommsenstrasse 4, 01069, Dresden (Germany)
E-mail: xinliang.feng@tu-dresden.de

S. Fu,[+] Prof. M. Bonn, Dr. H. I. Wang
Max Planck Institute for Polymer Research
Ackermannweg 10, 55128, Mainz (Germany)
E-mail: wanghai@mpip-mainz.mpg.de

Dr. A. H. Khan, Prof. E. Brunner
Chair of Bioanalytical Chemistry, Technische Universität Dresden
01062, Dresden (Germany)

Y. Zhang, Dr. M. Položij, Prof. T. Heine
Faculty of Chemistry and Food Chemistry, Technische Universität Dresden
Mommsenstrasse 4, 01069, Dresden (Germany)

Dr. A. Dianat, Prof. G. Cuniberti
Chair of Material Science and Nanotechnology, Faculty of Mechanical Science and Engineering, Technische Universität Dresden, Dresden (Germany)

Dr. Z. Liao
Fraunhofer Institute for Ceramic Technologies and Systems (IKTS)
01109, Dresden (Germany)

Prof. X. Feng
Department of Synthetic Materials and Functional Devices, Max-Planck Institute of Microstructure Physics
06120 Halle (Germany)

[+] These authors contributed equally to this work.

bonds.[20a,b,21] However, the *E*/*Z* selectivity of aryl ylide-based Wittig reactions is generally poor.[21,22] To control the stereoisomerism of the Wittig reaction, we tailor the high *E* selectivity through (i) elevating temperature as an additional energy source to provide the thermodynamic driving force; (ii) screening proper catalyst to obtain more stable intermediates with preferred geometry and associated facial selectivity during C=C bond formation. The optimized Wittig reaction is then performed for 2D polymerization, and four different V-2D-COFs are successfully synthesized by combining 2,3,8,9,14,15-hexa(4-formylphenyl)diquinoxalino [2,3-*a*:2′,3′-*c*]phenazine (HATN-6CHO) and four ylides. The resultant V-2D-COFs present crystalline dual-pore structures and robust unsubstituted vinylene-linkages with high chemical stability. V-2D-COFs synthesized by the Wittig reaction method show comparable crystallinity to their counterparts prepared by the widely used Knoevenagel reaction. Remarkably, ultrafast THz spectroscopy reveals excellent charge transport properties at the microscopic level, such as long scattering times (≈40–110 fs) and high charge mobilities (0.6–10.3 $cm^2 V^{-1} s^{-1}$) in V-2D-COFs.

The Wittig reaction generally occurs under strong basic conditions such as *n*-butyl lithium (n-BuLi) or sodium hydride (NaH) at low temperatures (below 0 °C), resulting in mainly (*Z*)-alkenes due to unstable intermediates.[23] It was reported that Cs^+ stabilizes the intermediates by forming a five- or six-membered cyclic transition state.[9,15,16] Thus Cs_2CO_3 was implemented in a model Wittig reaction between benzaldehyde (**1**) and [(1,1′-biphenyl)-4,4′-diylbis(methylene)] bis(triphenylphosphonium chloride) (BDMBT) (**2**) to synthesize 4,4′-di((*E*)-styryl)-1,1′-biphenyl (**3**) with high yield at 130 °C in the solvent mixture of 1,3-dimethyl-2-imidazolidinone (DMI) and mesitylene (Mes) (Figure 1a). The mass spectrometry (MS) (Figure S2) and ^{1}H NMR spectrum (Figure 1b) confirmed the formation of compound **3** with *trans* C=C configuration.[15,23]

To gain insight into the (*E*/*Z*) selectivity, in situ time-dependent ^{1}H NMR studies of model reaction were carried out in DMSO-d_6. From the peak area ratio between 7.1–7.3 ppm (*E*) and 6.6 ppm (*Z*), the high *trans*-selectivities of model reaction (**1**+**2**) were achieved with Cs_2CO_3 as catalyst at 80 °C (83.3 %) and 100 °C (89.1 %), while no considerable product was observed at 50 °C (Figure 1c, S3 and S4). This result suggests that elevated temperature is necessary to provide energy to impart reaction directionality (kinetic) to achieve high selectivity. Moreover, high *trans*-selectivities of 88.5 %, 83.0 % and 90.1 % were also observed for other model reactions between benzaldehyde (**1**) and different triphenyl phosphonium ylides such as 1,4-xylylenebis (triphenylphosphonium chloride) (XTPC, **9**, Supporting Information), (2,5-dimethyl-1,4-phenylene)bis(triphenylphosphonium chloride) (DPBTC, **11**, Supporting Information) and 1,1′-[[2,2′-bipridine]-4,4′-diylbis(methylene)]bis[1,1,1-triphenylphosphonium bromine] (BPDMBT, **7**, Figure S5–7), respectively (see Figure S8–S11). In contrast, the model reactions using NaOH as catalyst at 80 °C presented only ca. 20 % *trans*-selectivity (Figure S12). Thus, both the proper catalyst and elevated temperature are crucial to impart high *trans*-selectivity to the aryl ylide-based Wittig reaction.

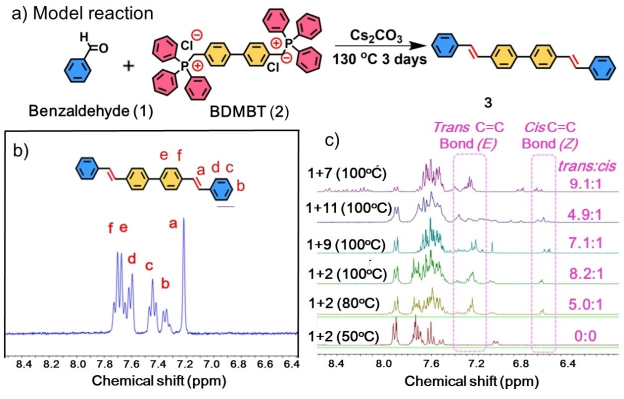

Figure 1. a) Schematic diagram of the model reaction to obtain product **3**. b) ^{1}H NMR spectrum of model product **3** ($C_2D_2Cl_4$, 80 °C). c) In situ high-temperature NMR study of the model reaction (**1**+**2**) at different temperatures (50 °C, 80 °C and 100 °C) and reactions between **1** and various ylides (**7, 9**, and **11**), respectively, at 100 °C after 2 h reaction.

Next, we synthesized the linear conjugated polymer poly(*p*-biphenylenevinylene) with a high yield (87 %) using Wittig polycondensation by combining terephthalaldehyde (**4**) and compound **2** (Figure 2a). The *m*/*z* ratio with one repeating unit of 280 and detectable molecular weights of 5463 $g mol^{-1}$ from the MS spectrum (Figure S18) indicate an efficient Wittig polymerization.[25] The chemical structure of the linear polymer was further confirmed by Fourier transform infrared (FTIR) spectroscopy (Figure S19). The strong intensity of the peak at 968 cm^{-1} in the FT-IR spectrum of the CPs also suggested the dominant *trans* C=C.[26] Notably, linear polymers have also been synthesized in the past (starting from 1960s) using Wittig reaction, further demonstrating the validity of Wittig polycondensation.[27]

Moreover, we had synthesized 2D CPs using the Wittig polycondensation. Interestingly, ultrahigh *E* selectivity (≈100 %) was observed for the 2D polymerization reaction between HATN-6CHO and compound **2** at 100 °C, which was identified by in situ time-dependent NMR study (Figure S20). Afterward, four vinylene-linked V-2D-COFs, namely V-2D-COF-W1 (V-2D-COF-HATN-BD), V-2D-COF-W2 (V-2D-COF-HATN-XT), V-2D-COF-W3 (V-2D-COF-HATN-DP) and V-2D-COF-W4 (V-2D-COF-HATN-BP) were synthesized between HATN-6CHO and four

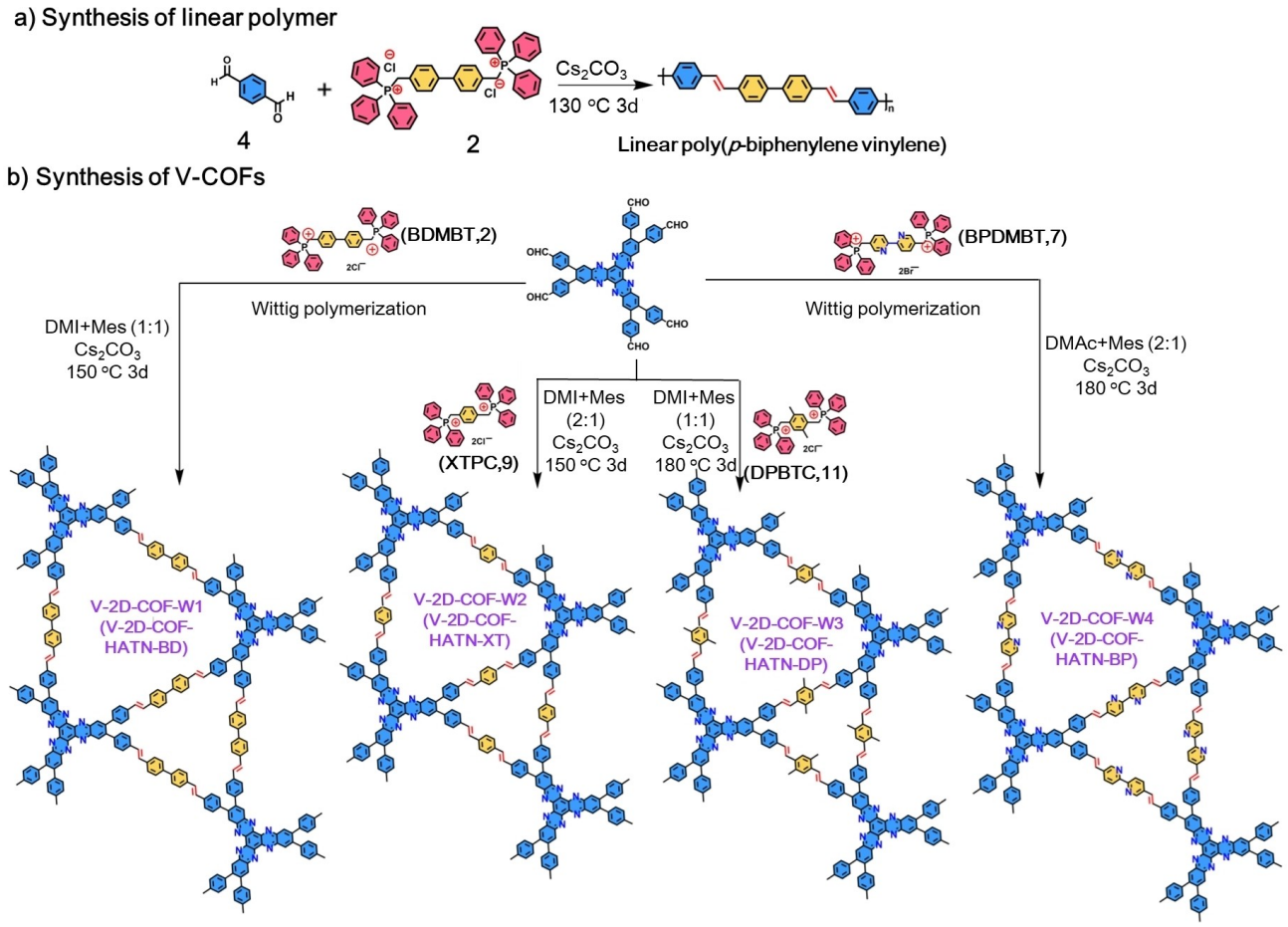

Figure 2. Synthesis of four V-2D-COFs through the Wittig 2D polycondensation.

various ylide salts including BDMBT(**2**), XTPC(**9**), DPBTC-(**11**) and BPDMBT(**7**), respectively (Figure 2b, S21–S24). The optimized synthesis of representative V-2D-COF-W1 was carried out by Cs_2CO_3-catalyzed Wittig condensation in a mixture of DMI/Mes = 1/1 at 150 °C. Tables S1–S4 summarize the reaction conditions.

The chemical structures of V-2D-COFs were examined by multiscale analytical methods. The signals at $\delta \approx 138$ and 132 ppm in ^{13}C cross-polarization magic angle spinning (CP-MAS) NMR spectra illustrate the vinylene-linkage formation in V-2D-COFs (Figure 3a).[14] Only very weak peak

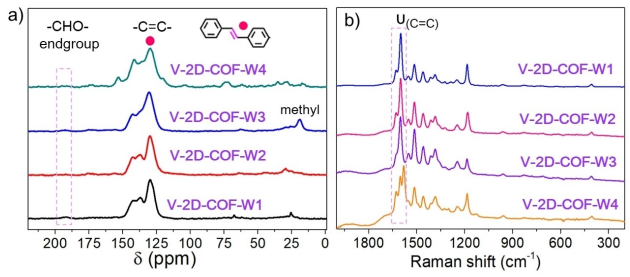

Figure 3. a) ^{13}C CP-MAS NMR spectra acquired at 2 ms contact time and b) Raman spectra of V-2D-COFs.

signal of –CHO group at around 180–200 ppm indicated a high conversion efficiency of –CHO from the HATN monomer.[15] With increasing the contact time, the C=O peak can be observed but the intensity remains low. This result suggests a relatively low density of C=O groups (Figure S25). Of note, there is no occurrence of [2+2] photocycloaddition between the COF layers, which is evidenced by the absence of significant signal around 40–50 ppm.[28] A characteristic band ranging from 1600–1650 cm^{-1} in both Raman (Figure 3b) and FTIR spectra (Figure S26 and 27) of V-2D-COFs further confirmed the formation of C=C bonds in their skeletons.[8,15,29] No P element from triphenylphosphine oxide or halide counterion elements was detected by X-ray photoelectron spectroscopy (XPS) (Figure S28).

The layered crystalline structures of V-2D-COFs were assessed by powder X-ray diffraction (PXRD). The first explicit reflection peaks of (100) (3.3–3.8°) and the additional peaks of (110) (6–7.5°) of the V-2D-COFs manifest a decent crystallinity of V-2D-COFs (Figure 4a–d). As an indicator of the average crystallite size, the full-width half-maximum (FWHM) of the (100) peaks of V-2D-COFs are ca. 0.96–1.03 (Figure S29), which are smaller than the same COF polymers (1.28–1.37) synthesized by HWE polycondensation, and well comparable with the counterpart of 2D-

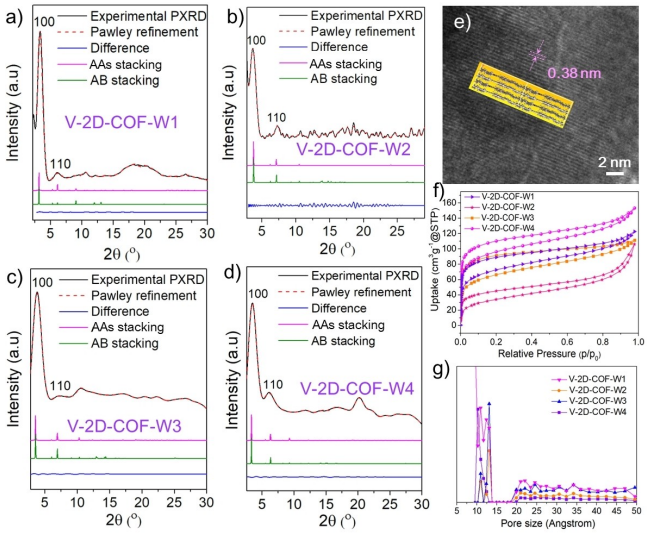

Figure 4. PXRD patterns of a) V-2D-COF-W1, b) V-2D-COF-W2, c) V-2D-COF-W3 and d) V-2D-COF-W4 with experimental (black) and Pawley-refinement (red), difference plot (blue), simulated PXRD with AAs stacking (pink) and AB stacking (green) modes. e) HR-TEM images of V-2D-COF-W1. The inset shows the side view of V-2D-COF-W1. f) N_2 adsorption and desorption isotherm curves and g) the pore size distribution profiles of V-2D-COFs.

CN-PPQV1 (1.06) synthesized by Knoevenagel polycondensation.[8,15] Moreover, Pawley refinement was performed (Table S5), and the crystal cell parameters of V-2D-COFs are shown in Table S6. High-resolution transmission electron microscopy (HR-TEM) image (Figure 4e) of representative V-2D-COF-W1 revealed a 2D stacking structure (ca. 0.38 nm) corresponding to the layer distance of V-2D-COF-W1, which is consistent with the simulated model. Of note, the (001) peaks of V-2D-COFs are not apparent in both the simulated and experimental PXRD spectra due to their slightly in-planar waved structures.

N_2 adsorption-desorption measurements examined the permanent porosity and surface area of V-2D-COFs at 77 K. A rise in the low-pressure range ($P/P_o = 0$–0.1) in the isotherm plots (Figure 4f) manifests a typical type-I N_2-sorption isotherm due to microporous structures of V-2D-COFs. The Brunauer–Emmett–Teller (BET) surface areas and the corresponding Langmuir surface areas of V-2D-COFs were concluded to be 118–333 $m^2 g^{-1}$ and 237–523 m^2/g, respectively (Table S7). Nonlocal density-functional theory (NLDFT) calculations (Figure 4g) disclose their dual-pore structures (Table S7). Although the simulated slipped AA (AAs) and AB stacking models show similar PXRD patterns, the AAs stacking model is considered to be energetically more favorable than the AB stacking model in all the V-2D-COFs due to its lower energy. (Table S8). Combining stabilized energies of different stacking modes and BET pore size measurements, we reasonably infer that our V-2D-COFs follow AAs stacked modes with a small slip between layers because of the aromatic ring (Figure S30 and S31).[15] Besides, the representative V-2D-COF-W1 shows outstanding chemical stability in strong acid, strong base and organic solvents owing to the robust vinylene linkage (Figure S32).

The optoelectronic properties of V-2D-COFs were studied by ultraviolet-visible (UV/Vis) absorption and fluorescence (FL) spectroscopy. Optical band gaps ranging from 2.10 to 2.26 eV are derived for these V-2D-COFs (Figure S33a). Besides, Figure S34 shows that the in-plane structure is fully conjugated with delocalized electrons in the valence band maximum (VBM) across the vinylene linkage and a bit distorted benzene rings. Moreover, the electronic structures (Table S9) and corresponding density of state (DOS) of V-2D-COFs with slipped AA stacking (Figure S35), monolayer (Figure S36) and AB stacking (Figure S37) are calculated by DFT method.[30] The evident emission (Em) peaks (628.3–591.7 nm) of V-2D-COFs are observed (Figure S33b). Apparently, the relatively smaller band gap (2.18 eV) and significantly longer wavelength of emission peak (628.3 nm) of V-2D-COF-W1 compared to the counterpart COF (2D CCP HATN)[8] containing a twisted pendant –CN group on the vinylene linkage (band gap = 2.39 eV and Em = 564 nm) synthesized by Knoevenagel polycondensation underscores the enhanced π-electron delocalization of the unsubstituted vinylene-linkage.[8,15]

The delocalized orbitals render V-2D-COFs with potentially excellent charge transport properties (Figure S38–S40). We investigated the microscopic electrical transport properties of V-2D-COFs via optical-pump THz-probe (OPTP) spectroscopy.[31,32] Due to the transient nature of the electric field in the THz probe pulses (with a duration of ≈1 ps), photogenerated charge carriers are driven only over 10s of nm. As such, OPTP spectroscopy characterizes the charge transport properties of materials at the microscopic level.[30] This is in contrast to conventional electrical measurements (e.g. using field effect transistors), in which macroscopic electrical properties are provided. I_2-doping was applied to V-2D-COFs to enhance the electrical properties of COFs.[33,34] Following optical excitations, both pristine and I_2- doped V-2D-COFs exhibit very similar dynamics, with a rapid rise due to the free carrier injection followed by a quick decay (within 2 ps), presumably as a result of charge localization and/or electron-hole recombination (Figure 5a). We have measured the frequency-resolved THz photoconductivity of bare and I_2-doped V-2D-COF-W1 as representative examples, which can be well-described by the Drude–Smith (DS) model (see details in Supporting Information), as shown in Figure 5b. The fitting yields scattering times (τ) of 49 ± 8 and 110 ± 12 fs for the bare and I_2-doped V-2D-COF-W1 respectively.[33] With knowing the reduced electron-hole effective masses $m^* = 0.63\, m_0$ ($1/m^* = 1/m_e + 1/m_h$) from the DFT calculation (Table S10),[35] we estimate the charge mobilities ($\mu = e\tau/m^*(1+c)$) of bare and I_2-doped V-2D-COF-W1 in the dc limit to be ≈1.4 $cm^2 V^{-1} s^{-1}$ and 3.1 $cm^2 V^{-1} s^{-1}$, respectively. Note that the estimated mobilities show the same trend as the photoconductivity. This method to infer mobilities has been widely used in various nanomaterial systems[35] and is in good agreement with device-based characterizations.[36]

Moreover, I_2-doping enhanced photoconductivity was observed for various V-2D-COFs (Figure S41). The highest

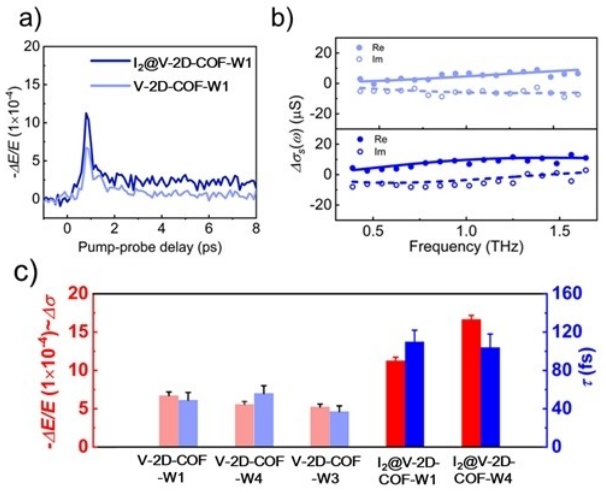

Figure 5. Time- and frequency-resolved THz photoconductivity of V-2D-COFs. a) THz photoconductivity dynamics and b) frequency-resolved complex sheet photoconductivity ($\Delta\sigma_s(\omega)$) of V-2D-COF-W1 with and without I_2 doping. The solid and dashed lines correspond to the Drude–Smith fits to the data. c) Comparison of the charge transport properties of various V-2D-COFs. The left and right Y-axes represent THz peak photoconductivities and inferred scattering times, respectively.

mobility of $\approx$10.3 $cm^2 V^{-1} s^{-1}$ was achieved for V-2D-COF-W3 (Figure S42). Overall, the V-2D-COFs show τ and μ in the ranges of $\approx$37–110 fs and 0.6–10.3 $cm^2 V^{-1} s^{-1}$, respectively (Figure 5c, Table S11 and S12), which are among the state-of-the-art conjugated COFs characterized by the same technique.[7,32–34,37] To establish the charge transport properties of our V-2D-COFs, we compare the photoconductivity of V-2D-COF-W1 to that of the same COF (2D PPQV2 in the original paper) prepared by other methods (e.g. via the HWE polycondensation[15]) and the counterpart COF (2D CCP HATN) by Knoevenagel polycondensation. Our V-2D-COF-1 shows higher THz photoconductivity than counterpart COFs by other synthesis routes (for both before and after of I_2 doping (Figure S43)), which may be tentatively attributed to lower crystallinity in 2D PPQV2 and decreased conjugation in 2D CCP HATN, respectively.

In conclusion, we demonstrated a novel synthetic strategy towards crystalline unsubstituted vinylene-linked 2D conjugated polymers using the Wittig reaction of aryl aldehydes with ylides. The attainment of the Wittig reaction's high (*E*)-alkene selectivity was confirmed by in situ/ex situ high-temperature NMR measurements and DFT calculations of model reactions. The chemically stable V-2D-COFs displayed moderate band gaps and red fluorescence. Ultrafast THz spectroscopy discloses state-of-the-art charge-transport properties in as-prepared and I_2-doped V-2D-COFs as a result of electron delocalization in the fully conjugated frameworks. More importantly, the V-2D-COFs synthesized by the Wittig reaction are characterized with higher charge carrier mobilities and thus a higher conjugation degree compared to their counterparts synthesized by the Knoevenagel and HWE reactions. We anticipate this work will inspire the development of novel 2D conjugated polymers with high charge-carrier mobilities, which holds great promise for the next-generation electronics and optoelectronics.

Acknowledgements

We thank the financial support from European Union's Horizon 2020 research and innovation programme (GrapheneCore3 881603), M-ERA.NET and Sächsisches Staatsministerium für Wissenschaft und Kunst (HYSUCAP 100478697 & Sonderzuweisung zur Unterstützung profilbestimmender Struktureinheiten), the ERC Consolidator Grant (T2DCP, NO. 819698), the DFG for the CRC 1415 (No. 417590517), Polymer-based Batteries (SPP 2248, RACOF-MMIS) and H2020-MSCA-ITN (ULTIMATE, No. 813036). S.F. and Y.Z. acknowledges fellowship support from the China Scholarship Council (CSC). We thank Dr. Guangbo Chen (TU Dresden) for the BET measurements and Dr. Zhiyong Wang (TU Dresden) for the TEM measurements. We thank Dr. Mingchao Wang for the helpful discussion. The author also acknowledges the Centre for Information Services and High Performance Computing (ZIH) in Dresden, Germany, for the provided computational resources. Open Access funding enabled and organized by Projekt DEAL.

Conflict of Interest

The authors declare no conflict of interest.

Data Availability Statement

The data that support the findings of this study are available from the corresponding author upon reasonable request.

Keywords: 2D Conjugated Polymer · Terahertz · Two-Dimensional Organic Framework · Vinylene-Linkage · Wittig Reaction

[1] S. Xu, M. Richter, X. Feng, *Acc. Mater. Res.* **2021**, *2*, 252.
[2] Y. Jin, Y. Hu, W. Zhang, *Nat. Chem. Rev.* **2017**, *1*, 0056.
[3] S. Xu, H. Sun, M. Addicoat, B. P. Biswal, F. He, S. Park, S. Paasch, T. Zhang, W. Sheng, E. Brunner, et al., *Adv. Mater.* **2021**, *33*, 2006274.
[4] X. Li, *Mater. Chem. Front.* **2021**, *5*, 2931.
[5] a) M. R. Rao, Y. Fang, S. de Feyter, D. F. Perepichka, *J. Am. Chem. Soc.* **2017**, *139*, 2421; b) E. Jin, J. Li, K. Geng, Q. Jiang, H. Xu, Q. Xu, D. Jiang, *Nat. Commun.* **2018**, *9*, 4143.
[6] a) Y. Zhao, H. Liu, C. Wu, Z. Zhang, Q. Pan, F. Hu, R. Wang, P. Li, X. Huang, Z. Li, *Angew. Chem. Int. Ed.* **2019**, *58*, 5376; *Angew. Chem.* **2019**, *131*, 5430; b) E. Jin, Z. Lan, Q. Jiang, K. Geng, G. Li, X. Wang, D. Jiang, *Chem* **2019**, *5*, 1632.
[7] E. Jin, S. Fu, H. Hanayama, M. A. Addicoat, W. Wei, Q. Chen, R. Graf, K. Landfester, M. Bonn, K. A. I. Zhang, et al., *Angew. Chem. Int. Ed.* **2022**, *61*, e202114059; *Angew. Chem.* **2022**, *134*, e202114059.

[8] S. Xu, G. Wang, B. P. Biswal, M. Addicoat, S. Paasch, W. Sheng, X. Zhuang, E. Brunner, T. Heine, R. Berger, et al., *Angew. Chem. Int. Ed.* **2019**, *58*, 849; *Angew. Chem.* **2019**, *131*, 859.
[9] M. Yu, R. Dong, X. Feng, *J. Am. Chem. Soc.* **2020**, *142*, 12903.
[10] E. Jin, M. Asada, Q. Xu, S. Dalapati, M. A. Addicoat, M. A. Brady, H. Xu, T. Nakamura, T. Heine, Q. Chen, et al., *Science* **2017**, *357*, 673.
[11] X. Zhuang, W. Zhao, F. Zhang, Y. Cao, F. Liu, S. Bi, X. Feng, *Polym. Chem.* **2016**, *7*, 4176.
[12] a) T. He, K. Geng, D. Jiang, *Trends Chem.* **2021**, *3*, 431; b) S. Xu, Z. Liao, A. Dianat, S. Park, M. A. Addicoat, Y. Fu, D. L. Pastoetter, F. G. Fabozzi, Y. Liu, G. Cuniberti, et al., *Angew. Chem. Int. Ed.* **2022**, *61*, e202202492; *Angew. Chem.* **2022**, *134*, e202202492.
[13] a) T. Jadhav, Y. Fang, W. Patterson, C.-H. Liu, E. Hamzehpoor, D. F. Perepichka, *Angew. Chem. Int. Ed.* **2019**, *58*, 13753; *Angew. Chem.* **2019**, *131*, 13891; b) H. Lyu, C. S. Diercks, C. Zhu, O. M. Yaghi, *J. Am. Chem. Soc.* **2019**, *141*, 6848; c) Z. Wang, Y. Yang, Z. Zhao, P. Zhang, Y. Zhang, J. Liu, S. Ma, P. Cheng, Y. Chen, Z. Zhang, *Nat. Commun.* **2021**, *12*, 1982.
[14] A. Acharjya, L. Longworth-Dunbar, J. Roeser, P. Pachfule, A. Thomas, *J. Am. Chem. Soc.* **2020**, *142*, 14033.
[15] D. L. Pastoetter, S. Xu, M. Borrelli, M. Addicoat, B. P. Biswal, S. Paasch, A. Dianat, H. Thomas, R. Berger, S. Reineke, et al., *Angew. Chem. Int. Ed.* **2020**, *59*, 23620; *Angew. Chem.* **2020**, *132*, 23827.
[16] D. L. Pastoetter, Y. Liu, M. A. Addicoat, S. Paasch, A. Dianat, D. Bodesheim, A. L. Waentig, S. Xu, M. Borrelli, A. Croy, et al., *Chem. Eur. J.* **2022**, *28*, e202104502.
[17] F. Haase, B. V. Lotsch, *Chem. Soc. Rev.* **2020**, *49*, 8469.
[18] a) N. Y. Shin, J. M. Ryss, X. Zhang, S. J. Miller, R. R. Knowles, *Science* **2019**, *366*, 364; b) A. Hölzl-Hobmeier, A. Bauer, A. V. Silva, S. M. Huber, C. Bannwarth, T. Bach, *Nature* **2018**, *564*, 240.
[19] M. Huang, L. Zhang, T. Pan, S. Luo, *Science* **2022**, *375*, 869.
[20] a) W. Carruthers, *Some modern methods of organic synthesis*, 3rd ed., Cambridge University Press, Cambridge, **1986**; b) R. W. Hoffmann, *Angew. Chem. Int. Ed.* **2001**, *40*, 1411; *Angew. Chem.* **2001**, *113*, 1457.
[21] R. Robiette, J. Richardson, V. K. Aggarwal, J. N. Harvey, *J. Am. Chem. Soc.* **2006**, *128*, 2394.
[22] B. E. Maryanoff, A. B. Reitz, *Chem. Rev.* **1989**, *89*, 863.
[23] H. Sakurai, T. Arai, *BCSJ* **2016**, *89*, 911.
[24] J. P. Perdew, K. Burke, M. Ernzerhof, *Phys. Rev. Lett.* **1996**, *77*, 3865.
[25] S. M. Weidner, S. Trimpin, *Anal. Chem.* **2008**, *80*, 4349.
[26] a) S. Pfeiffer, H.-H. Hörhold, *Synth. Met.* **1999**, *101*, 109; b) R. N. McDonald, T. W. Campbell, *J. Am. Chem. Soc.* **1960**, *82*, 4669.
[27] K. L. Brandon, P. G. Bentley, D. Bradley, D. A. Dunmur, *Synth. Met.* **1997**, *91*, 305.
[28] J. Heyd, G. E. Scuseria, M. Ernzerhof, *Chem. Phys.* **2003**, *118*, 8207.
[29] a) X. Yao, W. Zheng, S. Osella, Z. Qiu, S. Fu, D. Schollmeyer, B. Müller, D. Beljonne, M. Bonn, H. I. Wang, et al., *J. Am. Chem. Soc.* **2021**, *143*, 5654; b) R. Ulbricht, R. Kurstjens, M. Bonn, *Nano Lett.* **2012**, *12*, 3821; c) A. Tries, S. Osella, P. Zhang, F. Xu, C. Ramanan, M. Kläui, Y. Mai, D. Beljonne, H. I. Wang, *Nano Lett.* **2020**, *20*, 2993; d) R. Ulbricht, E. Hendry, J. Shan, T. F. Heinz, M. Bonn, *Rev. Mod. Phys.* **2011**, *83*, 543.
[30] G. Xing, W. Zheng, L. Gao, T. Zhang, X. Wu, S. Fu, X. Song, Z. Zhao, S. Osella, M. Martínez-Abadía, et al., *J. Am. Chem. Soc.* **2022**, *144*, 5042.
[31] E. Jin, K. Geng, S. Fu, M. A. Addicoat, W. Zheng, S. Xie, J.-S. Hu, X. Hou, X. Wu, Q. Jiang, et al., *Angew. Chem. Int. Ed.* **2022**, *61*, e202115020; *Angew. Chem.* **2022**, *134*, e202115020.
[32] M. Wang, M. Wang, H.-H. Lin, M. Ballabio, H. Zhong, M. Bonn, S. Zhou, T. Heine, E. Cánovas, R. Dong, et al., *J. Am. Chem. Soc.* **2020**, *142*, 21622.
[33] T. L. Cocker, D. Baillie, M. Buruma, L. V. Titova, R. D. Sydora, F. Marsiglio, F. A. Hegmann, *Phys. Rev. B* **2017**, *96*, 075311.
[34] Q. Zhang, M. Dai, H. Shao, Z. Tian, Y. Lin, L. Chen, X. C. Zeng, *ACS Appl. Mater. Interfaces* **2018**, *10*, 43595.
[35] a) W. Zheng, B. Sun, D. Li, S. M. Gali, H. Zhang, S. Fu, L. Di Virgilio, Z. Li, S. Yang, S. Zhou, et al., *Nat. Phys.* **2022**, *18*, 544; b) H. Shi, S. Fu, Y. Liu, C. Neumann, M. Wang, H. Dong, P. Kot, M. Bonn, H. I. Wang, A. Turchanin, et al., *Adv. Mater.* **2021**, *33*, 2105694.
[36] Z.-Y. Wang, L. Di Virgilio, Z.-F. Yao, Z.-D. Yu, X.-Y. Wang, Y.-Y. Zhou, Q.-Y. Li, Y. Lu, L. Zou, H. I. Wang, et al., *Angew. Chem. Int. Ed.* **2021**, *60*, 20483; *Angew. Chem.* **2021**, *133*, 20646.
[37] a) E. Jin, K. Geng, S. Fu, S. Yang, N. Kanlayakan, M. A. Addicoat, N. Kungwan, J. Geurs, H. Xu, M. Bonn, et al., *Chem* **2021**, *7*, 3309; b) M. Wang, M. Ballabio, M. Wang, H.-H. Lin, B. P. Biswal, X. Han, S. Paasch, E. Brunner, P. Liu, M. Chen, et al., *J. Am. Chem. Soc.* **2019**, *141*, 16810.

Manuscript received: July 4, 2022
Accepted manuscript online: September 25, 2022
Version of record online: ■■, ■■

Communications

Two-Dimensional Materials

Y. Liu, S. Fu, D. L. Pastoetter, A. H. Khan, Y. Zhang, A. Dianat, S. Xu, Z. Liao, M. Richter, M. Yu, M. Položij, E. Brunner, G. Cuniberti, T. Heine, M. Bonn, H. I. Wang,* X. Feng* ——— **e202209762**

Vinylene-Linked 2D Conjugated Covalent Organic Frameworks by Wittig Reactions

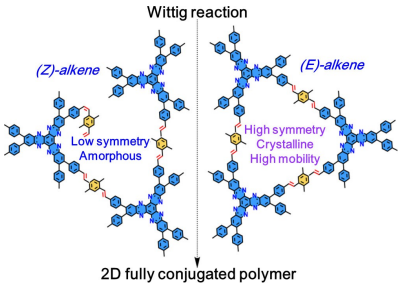

The Wittig reaction is demonstrated as novel synthetic strategy for the synthesis of crystalline unsubstituted vinylene-linked 2D conjugated covalent organic frameworks through the attainment of high (*E*)-alkene selectivity. Ultrafast THz spectroscopy discloses state-of-the-art charge-transport properties of as-prepared V-2D-COFs as a result of electron delocalization in the fully conjugated frameworks.